

1                                    **Supplementary figures for**  
2                                    **Quantifying the deviation of the tropical upper**  
3                                    **tropospheric temperature response to surface warming**  
4                                    **from a moist adiabat**

5                                    **Osamu Miyawaki<sup>1</sup>, Zhihong Tan<sup>2</sup>, Tiffany Shaw<sup>1</sup>, Malte Jansen<sup>1</sup>**

6                                    <sup>1</sup>Department of the Geophysical Sciences, The University of Chicago  
7                                    <sup>2</sup>Program in Atmospheric and Oceanic Sciences, Princeton University

---

Corresponding author: Osamu Miyawaki, [miyawaki@uchicago.edu](mailto:miyawaki@uchicago.edu)

**Table S1.** Overprediction in % of the moist adiabat across the model hierarchy for individual models used in this study. Blank data denote models for which data was not available in the corresponding model configuration.

	abrupt4 $\times$ CO <sub>2</sub>	amipF+4 $\times$ CO <sub>2</sub>	amipF	amip4K+4 $\times$ CO <sub>2</sub>	amip4K	aqua4K+4 $\times$ CO <sub>2</sub>	aqua4K
ACCESS1-0	10.6	–	–	–	–	–	–
ACCESS1-3	27.5	–	–	–	–	–	–
bcc-csm1-1	23.1	19.4	15.6	22.8	18.4	–	–
bcc-csm1-1-m	32.3	–	–	–	–	–	–
BNU-ESM	27.1	–	–	–	–	–	–
CanESM2	25.5	15.8	14.0	15.6	13.5	–	–
CCSM4	26.4	22.8	22.9	23.8	23.9	23.6	22.6
CNRM-CM5	46.9	40.3	33.3	40.2	31.9	52.0	40.1
CNRM-CM5-2	46.4	–	–	–	–	–	–
CSIRO-Mk3-6-0	28.0	–	–	–	–	–	–
FGOALS-g2	24.5	–	–	–	–	20.5	17.3
FGOALS-s2	35.5	–	–	–	–	–	–
GFDL-CM3	22.2	–	–	–	–	–	–
GFDL-ESM2G	31.4	–	–	–	–	–	–
GFDL-ESM2M	33.8	–	–	–	–	–	–
GISS-E2-H	23.8	–	–	–	–	–	–
GISS-E2-R	21.2	–	–	–	–	–	–
HadGEM2-ES	12.6	10.0	5.1	11.2	5.6	7.1	4.4
inmcm4	36.6	–	–	–	–	–	–
IPSL-CM5A-LR	27.1	21.0	21.5	21.1	21.7	22.4	23.2
IPSL-CM5A-MR	27.1	–	–	–	–	–	–
IPSL-CM5B-LR	13.4	12.3	12.0	13.1	12.7	–	–
MIROC-ESM	8.2	–	–	–	–	–	–
MIROC5	22.8	17.8	16.0	18.0	15.8	19.4	19.9
MPI-ESM-LR	16.5	16.0	8.3	18.5	9.5	–11.4	–17.3
MPI-ESM-MR	16.9	19.6	11.1	21.3	11.7	–9.3	–15.6
MPI-ESM-P	17.0	–	–	–	–	–	–
MRI-CGCM3	29.8	26.4	23.1	26.5	22.5	24.8	21.1
NorESM1-M	20.9	–	–	–	–	–	–
All model mean	25.3	20.1	16.6	21.1	17.0	16.6	12.9
AMIP-subset mean	23.7	20.1	16.6	21.1	17.0	16.1	12.3
Aqua-subset mean	24.8	21.7	17.6	22.6	17.8	16.6	12.9

**Table S2.** P-values of the T-test for the null hypothesis that the difference in mean overprediction between the abrupt4×CO<sub>2</sub> response and that of simpler models are indistinguishable. The mean difference and the 5–95% confidence interval are also shown. The difference is statistically significant for all model configurations (p-value < 5%, indicated in bold).

	Lower Bound	Mean	Upper Bound	p-value
abrupt4×CO <sub>2</sub> –amipF	4.85	7.10	9.35	<b>3.58E-5</b>
abrupt4×CO <sub>2</sub> –amip4K	4.01	6.69	9.37	<b>2.41E-4</b>
abrupt4×CO <sub>2</sub> –aqua4K	2.61	11.96	21.31	<b>0.0185</b>

**Table S3.** Overprediction in % of the moist adiabat across the model hierarchy for various types of the moist adiabat. Three types of moist adiabats are shown here following the definitions in the AMS glossary. *Standard*: The limit of a moist pseudoadiabat when  $r_v \ll 1$  (AMS, cited 2020: Moist-adiabatic lapse rate). *Pseudo*: Moist pseudoadiabat, which assumes that all condensates precipitate immediately (AMS, cited 2020: pseudoadiabatic lapse rate). *Reversible*: Reversible moist-adiabat, which assumes that all condensates remain in the rising parcel (AMS, cited 2020: reversible moist-adiabatic process).

	Standard	Pseudo	Reversible
abrupt4×CO <sub>2</sub>	25.3	30.5	24.7
amipF	16.6	21.6	15.4
amip4K	17.0	22.1	15.9
aqua4K	12.9	18.6	11.9
GFDLaqua4K	14.2	19.9	13.5
GFDLrce4K	11.6	16.8	11.1

**Table S4.** P-values of the T-test for the null hypothesis that the difference in mean overprediction averaged over 10°N/S and averaged only over regions of strong mean ascent ( $\omega_{500} < -35$  hPa/d, indicated with an asterisk below) are indistinguishable. The mean difference and the 5–95% confidence interval are also shown. The difference is statistically significant for model configurations that have zonally-asymmetric circulations. (p-value < 5%, indicated in bold).

	Lower Bound	Mean	Upper Bound	p-value
abrupt4×CO <sub>2</sub> –abrupt4×CO <sub>2</sub> *	3.89	6.10	8.30	<b>0.0000</b>
amipF–amipF*	3.92	7.27	10.63	<b>0.0007</b>
amip4K–amip4K*	0.88	3.62	6.36	<b>0.0146</b>
aqua4K–aqua4K*	–3.76	–0.21	3.35	0.8973

**Table S5.** P-values of the T-test for the null hypothesis that the difference in mean overprediction between the combined surface warming plus the direct CO<sub>2</sub> response and only the surface warming response are indistinguishable. The mean difference and the 5–95% confidence interval are also shown. The difference is statistically significant for all model configurations (p-value < 5%, indicated in bold).

	Lower Bound	Mean	Upper Bound	p-value
amipF+4×CO <sub>2</sub> *–amipF*	1.53	3.63	5.72	<b>0.0032</b>
amip4K+4×CO <sub>2</sub> *–amip4K*	1.54	3.94	6.33	<b>0.0043</b>
aqua4K+4×CO <sub>2</sub> *–aqua4K*	0.94	3.15	5.35	<b>0.0110</b>

**Table S6.** Same as Table S3 but overprediction is evaluated only over regions of strong mean ascent ( $\omega_{500} < -35$  hPa/d, indicated by an asterisk). This filter is not applied to GFDLrce4K as the RCE configuration lacks a climatological large-scale circulation.

	Standard	Pseudo	Reversible
abrupt4 $\times$ CO <sub>2</sub> *	19.3	24.6	18.3
amipF*	9.3	14.4	7.7
amip4K*	13.4	18.6	11.9
aqua4K*	13.1	18.8	11.9
GFDLaqua4K*	13.2	18.7	12.4
GFDLrce4K*	—	—	—

**Table S7.** Same as Table S1 except overprediction is evaluated only over regions of strong mean ascent ( $\omega_{500} < -35$  hPa/d, indicated by an asterisk).

	abrupt4 $\times$ CO $_2^*$	amipF+4 $\times$ CO $_2^*$	amipF*	amip4K+4 $\times$ CO $_2^*$	amip4K*	aqua4K+4 $\times$ CO $_2^*$	aqua4K*
ACCESS1-0	7.6	—	—	—	—	—	—
ACCESS1-3	23.2	—	—	—	—	—	—
bcc-csm1-1	11.6	5.9	1.4	12.3	7.4	—	—
bcc-csm1-1-m	29.3	—	—	—	—	—	—
BNU-ESM	27.9	—	—	—	—	—	—
CanESM2	10.4	6.2	5.9	9.3	9.1	—	—
CCSM4	29.4	22.2	22.1	26.7	26.6	23.2	21.7
CNRM-CM5	46.2	39.5	32.1	39.8	31.4	50.3	43.0
CNRM-CM5-2	45.5	—	—	—	—	—	—
CSIRO-Mk3-6-0	9.6	—	—	—	—	—	—
FGOALS-g2	22.4	—	—	—	—	19.6	16.9
FGOALS-s2	24.6	—	—	—	—	—	—
GFDL-CM3	18.4	—	—	—	—	—	—
GFDL-ESM2G	30.5	—	—	—	—	—	—
GFDL-ESM2M	31.6	—	—	—	—	—	—
GISS-E2-H	19.8	—	—	—	—	—	—
GISS-E2-R	18.2	—	—	—	—	—	—
HadGEM2-ES	8.1	8.2	4.5	10.7	6.5	5.2	4.7
inmcm4	24.2	—	—	—	—	—	—
IPSL-CM5A-LR	21.0	11.0	8.6	21.5	19.5	21.9	21.8
IPSL-CM5A-MR	19.2	—	—	—	—	—	—
IPSL-CM5B-LR	6.1	11.0	−2.0	3.6	3.4	—	—
MIROC-ESM	−11.3	—	—	—	—	—	—
MIROC5	10.5	10.4	8.3	14.2	11.9	11.0	11.4
MPI-ESM-LR	11.1	9.6	1.8	13.1	4.4	−4.0	−9.9
MPI-ESM-MR	10.0	13.0	4.4	16.2	6.6	−5.4	−10.4
MPI-ESM-P	12.2	—	—	—	—	—	—
MRI-CGCM3	17.9	18.2	15.7	23.4	20.6	24.1	18.6
NorESM1-M	23.2	—	—	—	—	—	—
All model mean	19.2	13.0	9.3	17.3	13.4	16.2	13.1
AMIP-subset mean	16.6	13.0	9.3	17.3	13.4	15.8	12.6
Aqua-subset mean	19.5	16.5	12.2	20.7	15.9	16.2	13.1

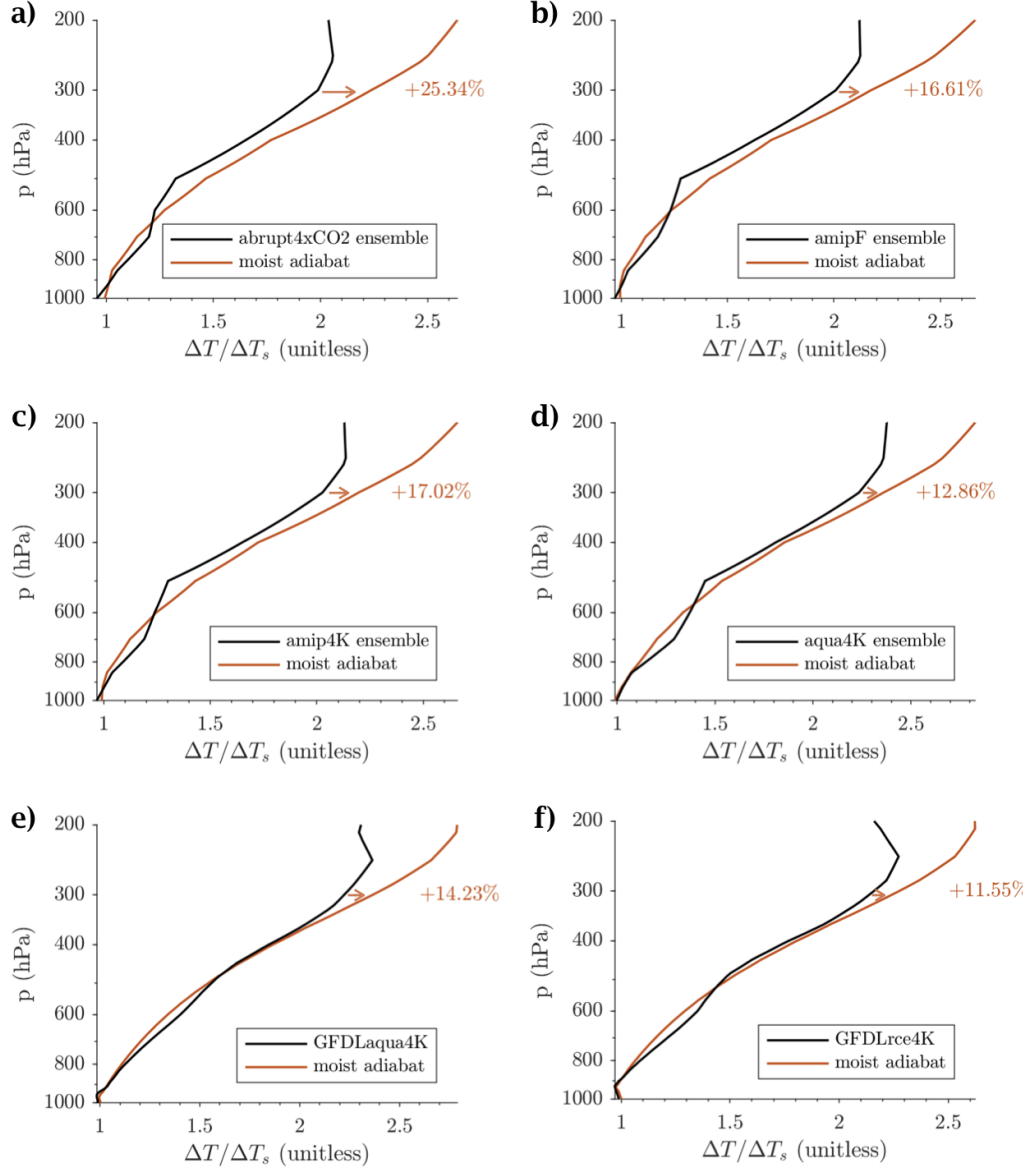


**Figure S1.** a) Vertical structure of the temperature response over the tropics (defined as  $10^{\circ}\text{N/S}$ ) for the CMIP5 multi-model mean (black) and the prediction based on a moist adiabat (orange). The moist adiabat overpredicts the CMIP5 response by 25.34% at 300 hPa. b)–d) are the same for the amipF, amip4K, and aqua4K multi-model mean responses, respectively. e) and f) are the same for GFDLaqua4K and GFDLrce4K responses.

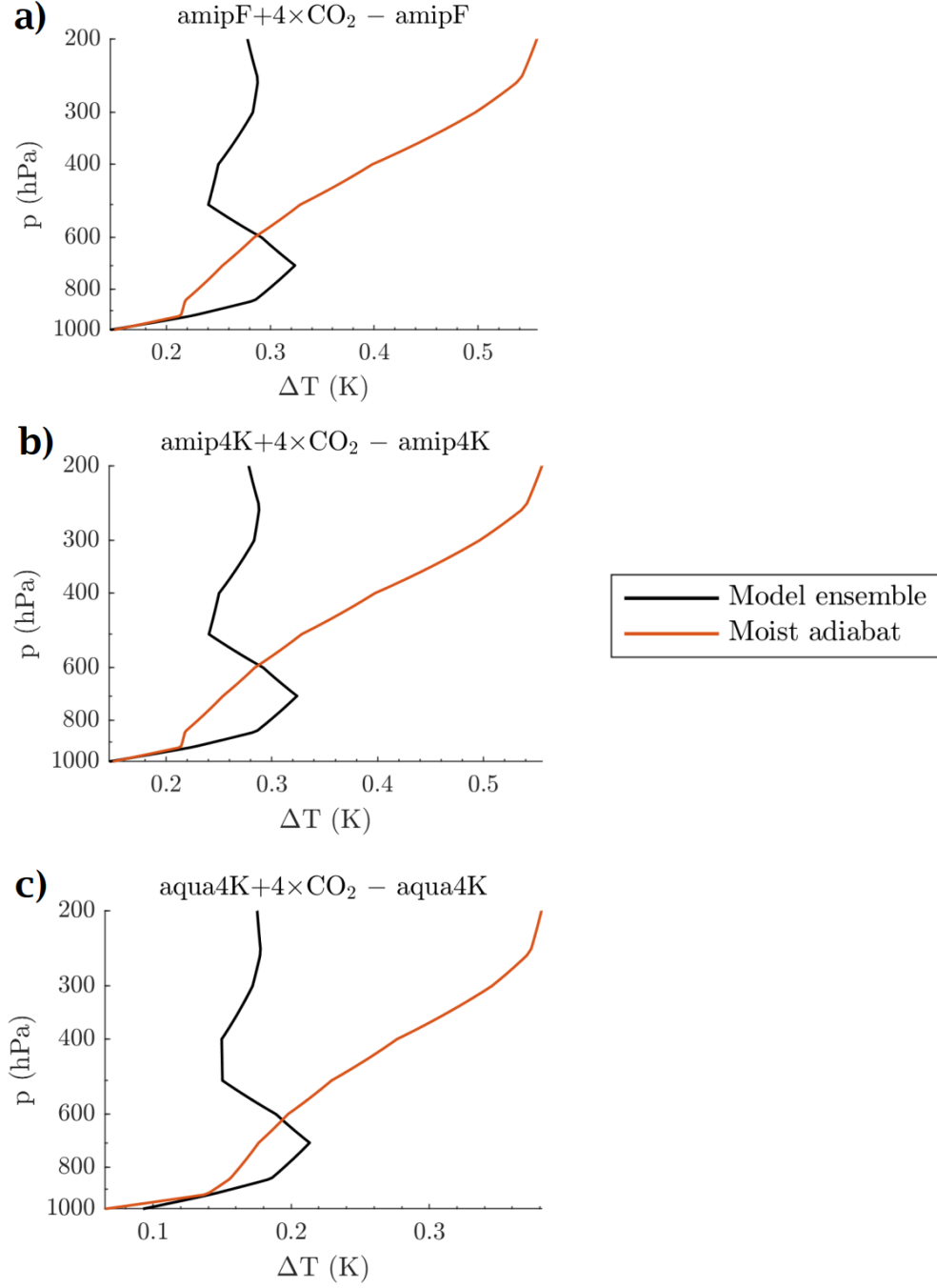


**Figure S2.** a) Vertical structure of the difference in multi-model mean temperature response between amipF+4×CO<sub>2</sub> and amipF (black) and the corresponding moist adiabatic prediction (orange). While the warming due to the direct effect of CO<sub>2</sub> is approximately uniform with height in the multi-model mean, the moist adiabat predicts amplified warming aloft. b) and c) are the same for the differences between amip4K+4×CO<sub>2</sub> and amip4K and aqua4K+4×CO<sub>2</sub> and aqua4K, respectively.

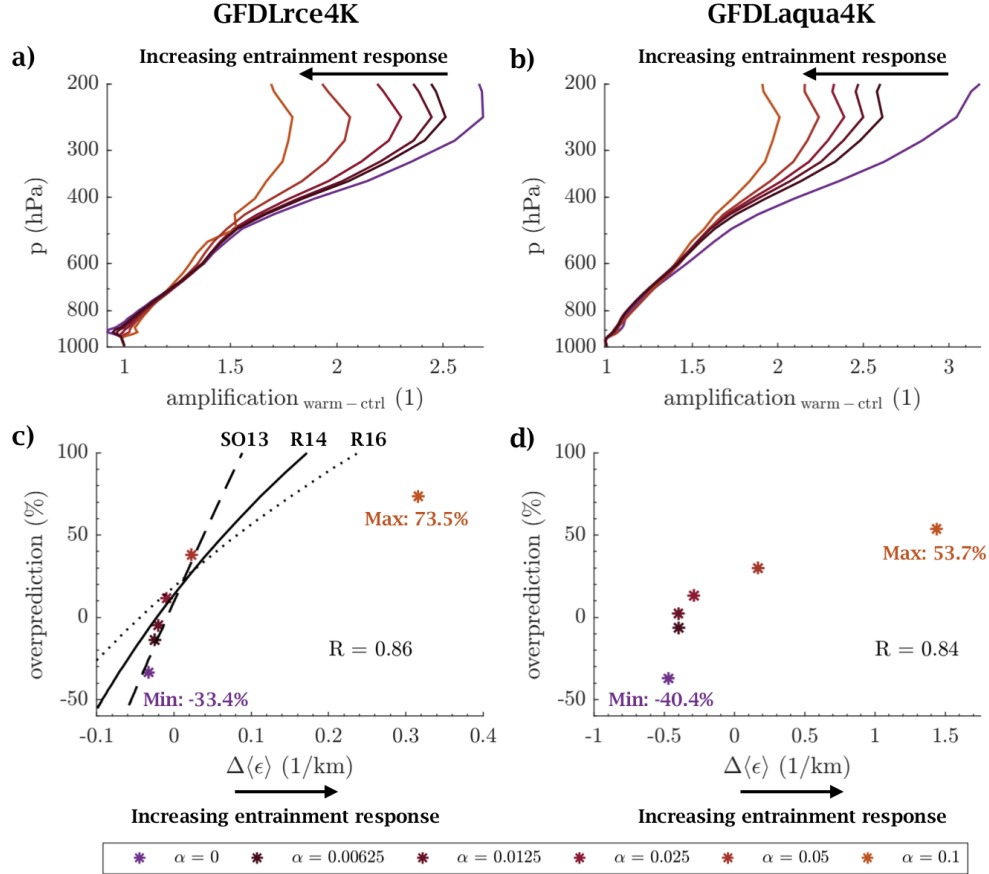


**Figure S3.** Temperature responses simulated in GFDL where the Tokioka parameter  $\alpha$  is held fixed at 0.025 for the control climate and varied as shown only for the warm climate. The amplified warming in the upper troposphere weakens when the entrainment strengthens with warming in a) GFDLrce4K and b) GFDLaqua4K. Overprediction of the moist adiabats scales with the response of entrainment in both c) GFDLrce4K and d) GFDLaqua4K. The deviation as predicted by zero-buoyancy bulk-plume models of Singh and O’Gorman (2013) (labeled SO13), Romps (2014) (R14), and Romps (2016) (R16) are shown as black lines in panel c.



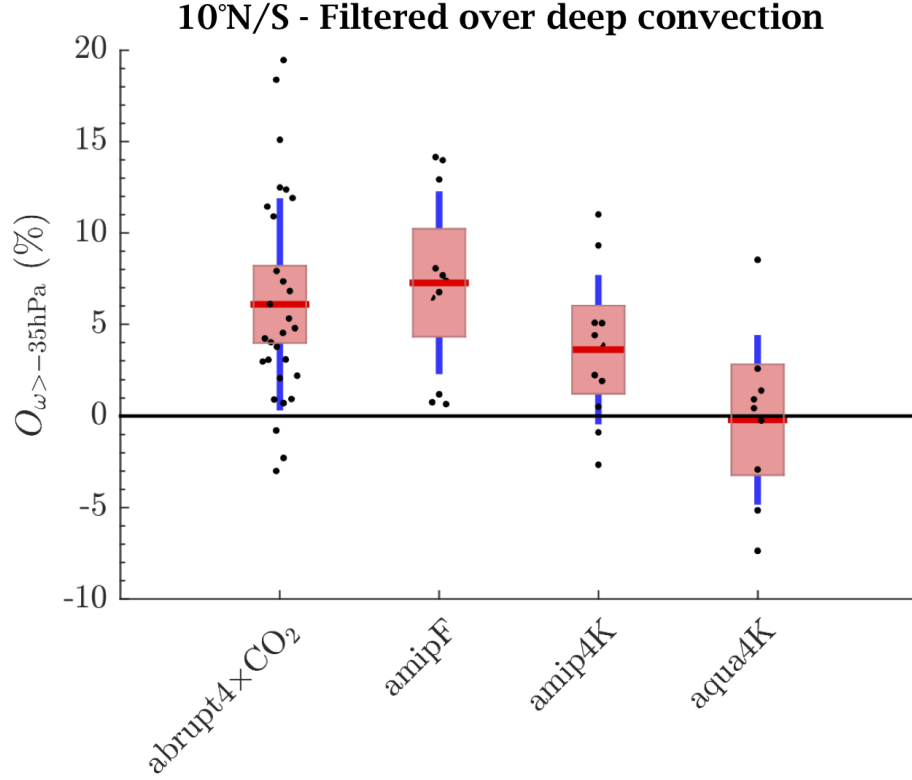


**Figure S4.** The difference between overprediction averaged over 10°N/S and overprediction averaged only over regions of climatological deep convection ( $\omega_{500} < -35$  hPa/d) for each model across the model hierarchy (black dots). The mean difference in overprediction is denoted by the red line. The red box shows the 5–95% confidence interval of the mean. The blue line shows one standard deviation of the distribution.

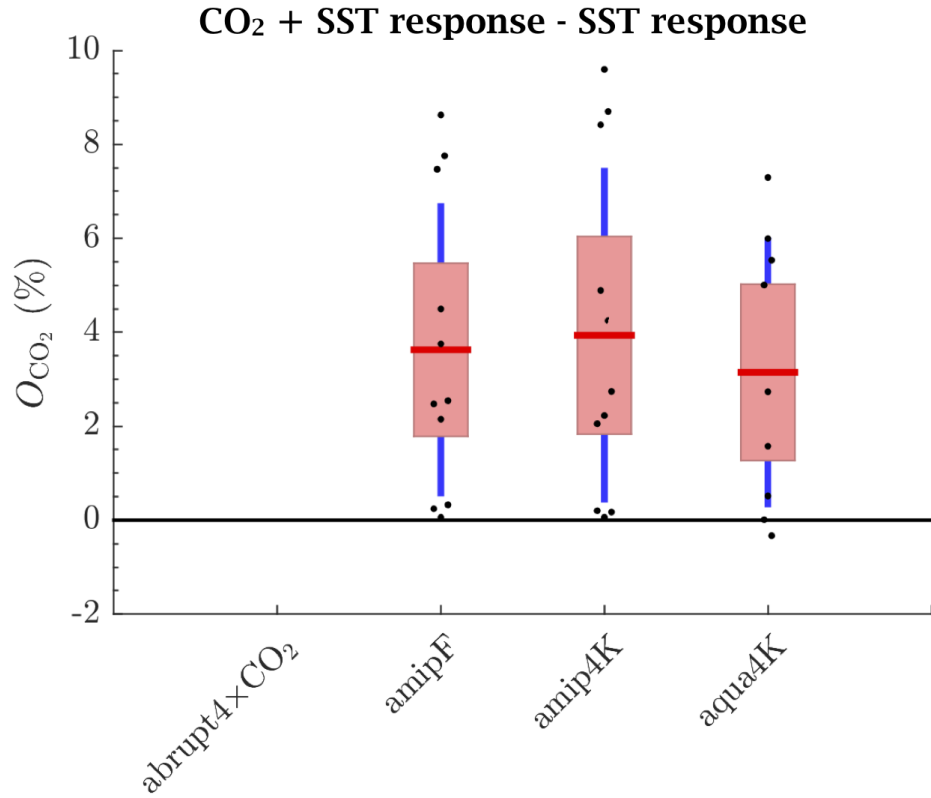


**Figure S5.** The difference in overprediction between the combined surface warming plus the direct CO<sub>2</sub> response and only the surface warming response for each model across the model hierarchy (black dots). The mean difference in overprediction is denoted by the red line. The red box shows the 5–95% confidence interval of the mean. The blue line shows one standard deviation of the distribution.